Available online at www.sciencedirect.com
SCIENCE DIRECT®
Journal of Chromatography A, 988 (2003) 205–218
JOURNAL OF CHROMATOGRAPHY A
www.elsevier.com/locate/chroma

Influence of pressure on the chromatographic behavior of insulin variants under nonlinear conditions

Xiaoda Liu[a,b,1], Pawel Szabelski[a,b,2], Krzysztof Kaczmarski[c], Dongmei Zhou[a,b], Georges Guiochon[a,b,*]

[a]*Department of Chemistry, The University of Tennessee, Buchler Hall, Knoxville, TN 37996-1600, USA*
[b]*Division of Chemical Sciences, Oak Ridge National Laboratory, Oak Ridge, TN, USA*
[c]*Faculty of Chemistry, Rzeszów University of Technology, 35-959 Rzeszów, Poland*

Received 4 October 2002; received in revised form 18 December 2002; accepted 20 December 2002

Abstract

The effect of pressure on the chromatographic behavior of two insulin variants in RPLC was investigated on a YMC-ODS C_{18} column, under nonlinear conditions. The adsorption isotherm data of porcine insulin and Lispro were measured at average column pressures ranging from 52 to 242 bar. These data fit well to the Toth and the bi-Langmuir isotherm models. The saturation capacity increases rapidly with increasing pressure while the affinity (or equilibrium) constant and the parameter characterizing the surface heterogeneity decrease. It is noteworthy that the distribution coefficient of the insulin variants increases with increasing pressure whereas their equilibrium constant b decreases for porcine insulin and increases for Lispro. The association constant b_{ds}, which characterizes the adsorption and desorption equilibrium of insulin in the system, increases with increasing pressure. The excellent agreement between the experimental overloaded profiles recorded under different pressures and those calculated using the POR model suggests that the chromatographic behavior of insulin is controlled more by equilibrium thermodynamics than by the mass transfer kinetics. The latter seems to be nearly independent of the average column pressure. Thus, increasing the average column pressure is an efficient, albeit costly, way to increase the loading capacity of the column, hence the production rate in preparative chromatography.
© 2003 Elsevier Science B.V. All rights reserved.

Keywords: Pressure-induced retention; Pore diffusion; Nonlinear chromatography; Adsorption isotherms; Insulin

1. Introduction

Pressure is an important thermodynamic parameter in solution investigations. It has proven to be a powerful tool in studies of protein structures and of their molecular interactions or associations [1–4]. High pressures (1–2 kbar) combined with low, non-denaturing concentrations of guanidine hydrochloride, foster the desaggregation and refolding of denatured and/or aggregated recombinant proteins

*Corresponding author. Tel.: +1-865-974-0733; fax: +1-865-974-2667.
E-mail address: guiochon@novell.chem.utk.edu (G. Guiochon).
[1]Present address: Beijing Institute of Transfusion Medicine, 27(9) Taiping Road, Beijing 100850, China.
[2]Present address: Department of Theoretical Chemistry, Maria Curie-Sklodowska University, pl. M.C.-Sklodowskiej 3, 20-031 Lublin, Poland.

0021-9673/03/$ – see front matter © 2003 Elsevier Science B.V. All rights reserved.
doi:10.1016/S0021-9673(03)00002-5

[5]. In an intermediate range, the main effect of pressure is to shift the position of the absolute minimum of the free energy of the protein energy landscape [6]. The elastic relaxation of the structural response of the protein–solvent system to moderate pressure variations is characterized by small changes in interatomic distances, changes that are reversible when the pressure is released, but that are not homogeneous throughout the protein structure. These changes affect essentially the distances between groups that are brought close by molecular interaction forces, not the actual bond lengths. In some cases, pressure and temperature play opposite roles: it has been observed in several proteins that a moderate pressure stabilizes against heat denaturation [7]. Proteins are stable in their native state inside an elliptic diagram in the $p–T$ plane [8]. To some extent, an increase in temperature could stabilize them against pressure denaturation [9]. Pressure-induced unfolding is considerably slower than temperature-induced unfolding [10].

Monte Carlo simulations showed that the desolvation barrier increases with increasing pressure, resulting in an increase of the roughness of the energy landscape [11]. Generally, simulations of the behavior of solvated proteins show that protein–solvent interactions are energetically more favorable under a high pressure than at atmospheric pressure. At the same time, the energy of protein–protein interactions increases with increasing pressure, due to moderate deformations of the bond angles and distances in the protein molecules. The more favorable interactions between protein and solvent molecules at high pressure are accompanied by an increase in the number of protein–solvent hydrogen bonds that are formed [12]. A decrease of the positional fluctuations of the atoms with increasing pressure was also observed. The mobility of the protein backbone was not affected, the effect being important mostly for the side chains [13]. An increasing pressure has a dampening effect on the amplitude of atomic oscillations, effect which is analogous to the one produced by a decrease of the temperature.

The compressibilities of all the amino acids are the same within 20%. The most compressible of them are the hydrophobic valine, leucine, and isoleucine while the least compressible ones are the charged amino acids glycine and aspartic acid. Proteins do not respond to a change in pressure in a uniform and homogeneous way. Different regions or substructures within the protein compress to a different extent [12]. Both the thermal expansion and the compressibility of proteins are composed of two main contributions, those of the cavities and the hydration terms. Under moderate pressures (below 1 to 3 kbar), one may assume that the compression of the cavities and an increased size of the solvation shell are the main effects [14]. Pressures of the order of 1000 to 4000 bar have been reported to cause the reversible dissociation of a number of oligomeric protein complexes, without causing great changes in the structure of the individual proteins [15]. Investigations of the pressure-induced dissociation of antigen–antibody complexes have shown that complexes having a strong electrostatic character are poorly sensitive to pressure variations, due to electrostriction effects, while more hydrophobic complexes exhibit a high pressure sensitivity [16].

McGuffin and Evans [17] observed a significant pressure dependence of the retention factors of the components of a homologous series in RP-HPLC. The relative variation of the partial molar volume of a methylene group upon adsorption, $\Delta V_{CH_2}/V_{CH_2}$, was shown to be close to 6% in a C_{18} bonded silica–methanol system [18]. Pressure was found to affect retention factors, chiral selectivity, and column efficiency for several enantiomeric separations, in different chromatographic systems [19]. For a series of *n*-fatty acids and a group of polynuclear aromatic hydrocarbons, increments of ΔV of the order of -14.1 ml/mol for an ethyl group and between -20 ml/mol and $+20$ ml/mol per aromatic ring were found on a polymeric C_{18} stationary phase at 30 °C. These increments are much lower on a monomeric C_{18} stationary phase with a low bonding density [20]. As for small molecules like nitrophenol, the volume change associated with ionization, partitioning on the stationary phase, and complexation with β-cyclodextrin on a C_{18} column is between -13 ml/mol and 10 ml/mol [21].

However, the effect of pressure is proportional to ΔV [18]. So, it is far more important for proteins such as insulin [22] or lysozyme [23] than for small molecules. The strong influence of the average column pressure on the retention of insulin [22] and lysozyme [23] is explained by the large value of ΔV

found, of the order of -100 ml mol^{-1} in both cases. It is probably related to the displacement of solvent and/or co-solvent molecules from the binding area more than to a change in the packing density of these proteins [23]. In the absence of the formation or breaking of covalent-bonds, the largest contribution is expected to be due to the change in solvation that accompanies changes in non-covalent molecular interactions. The mechanism also implicates modifications of the stationary phase through changes in its solvation with the components of the mobile phase. These changes affect the equilibrium process that controls solute retention.

The pressure/temperature dependence of the retention of insulin variants on a C_{18} bonded silica was studied under linear conditions by Szabelski et al. [24]. The value of ΔV_m for Lispro[3], human insulin, bovine insulin, and porcine insulin at 25 °C and 50 °C are all close to -102 ml/mol with water–acetonitrile (70:30, v/v) as the mobile phase. The influence of pressure on the retention of insulin under linear conditions was later studied at different mobile phase compositions to probe the mechanism of this effect [25]. ΔV_m was found to depend strongly on the acetonitrile concentration of the mobile phase.

In a previous paper, adsorption isotherm data were measured for insulin on a C_{18} bonded silica column under the conventional condition of the column outlet under atmospheric pressure [26]. These data were modeled and found to fit well to the Toth isotherm model. The pore diffusion model (POR) was used to calculate overloaded band profiles of insulin. Excellent agreement of these calculated profiles with the experimental data was observed. Later, the stoichiometric displacement model [27] was used to estimate the number of molecules displaced from the binding area and the influence of pressure on this number under linear conditions. However, a more detailed thermodynamic study of the retention mechanism requires the use of nonlinear data. In this paper, we report on a study of the influence of pressure on the adsorption behavior of insulin under nonlinear conditions. Particular attention is given to the influence of pressure on the saturation capacity of the column and to the parameters that affect it. The saturation capacity of an adsorbent or amount required to form a monolayer on its surface controls directly the production rate in preparative chromatography. This makes it a parameter of critical importance in this field, both from fundamental and practical perspectives.

[3]The structure of the C-terminal of the B chain of human insulin is: –Phe–Phe–Tyr–**Pro–Lys**–Thr–CO_2H. That of Lispro is –Phe–Phe–Tyr–**Lys–Pro**–Thr–CO_2H.

2. Theoretical

2.1. Volume change of solute upon adsorption

Both the protein and the bonded C_{18} groups of the stationary phase are solvated by the mobile phase, an aqueous solution of acetonitrile. According to the stoichiometric displacement model [27], the solvent molecules in the binding area will be displaced upon adsorption of the protein through hydrophobic interactions. The adsorption equilibrium process of the protein follows the reaction:

$$P + S \rightleftharpoons PS + zD_0 \tag{1}$$

The association equilibrium constant, b_{ds}, is defined by the equation:

$$b_{ds} = \frac{C_s[D_0]^Z}{C_m[S]} = K \cdot \frac{[D_0]^Z}{[S]} \tag{2}$$

where C_s and C_m are the concentrations of the protein in the stationary and the mobile phase at equilibrium, $[S]$ is the number of the binding sites available for the protein on the surface of the stationary phase, $[D_0]$ is the organic solvent concentration (molarity) in the mobile phase, Z is the number of organic solvent molecules displaced upon adsorption of one molecule of the protein. For a chromatographic separation carried out under isocratic conditions, the concentration of the organic solvent is constant and, in this case, we rewrite Eq. (2) as:

$$b = \frac{b_{ds}}{[D_0]^Z} = \frac{C_s}{C_m[S]} = K/[S] \tag{3}$$

where $K = C_s/C_m$ is the distribution coefficient of the protein between the stationary and the mobile phase and b is the affinity or apparent equilibrium

constant (a function of the mobile phase composition).

According to Eq. (2), the retention factor of the solute can be expressed as:

$$k = K\Phi = \frac{b_{ds}\Phi[S]}{[D_0]^Z} \tag{4}$$

where k is the solute retention factor and Φ the phase ratio. According to Eq. (3), the fractional surface coverage at equilibrium is given by:

$$\theta = \frac{C_s}{C_s + [S]} = \frac{bC_m[S]}{bC_m[S] + [S]} = \frac{bC_m}{1 + bC_m} \tag{5}$$

This is the equation of the Langmuir adsorption isotherm. Obviously, in writing Eq. (5), we assume the surface of the stationary phase to be homogeneous, which, as we show later, it is actually not. However, the energetic heterogeneity of the surface remains modest and the Langmuir model may be used as a first-order approximation to derive estimates of the physicochemical properties of the surface.

The distribution coefficient of the protein between the stationary and the mobile phase at infinite dilution can be derived from Eqs. (2) and (5) as:

$$K = bq_s = b_{ds}[S]/[D_0]^Z \tag{6}$$

The distribution coefficient depends on the association constant, the saturation capacity or number of adsorption sites on the surface, and the number of organic solvent molecules that are displaced upon protein adsorption.

In a chromatographic system, the solute retention is directly related to the equilibrium thermodynamics. The change in Gibbs free energy of the system is:

$$\Delta G = \Delta H - T\Delta S = -RT \ln K = -RT \ln (k/\phi) \tag{7}$$

where ΔG, ΔH and ΔS are the differences in molar Gibbs free energy, enthalpy and entropy, respectively, that are associated with the passage of one mole of solute from the mobile to the stationary phase, R is the universal gas constant, K the distribution constant of the solute between the stationary and the mobile phase, k is the solute retention factor, and ϕ is the phase ratio. The influence of pressure and temperature on the equilibrium of the solute between the two phases can be derived from the differential of the molar Gibbs free energy:

$$d(\Delta G) = \Delta V\, dP - \Delta S\, dT \tag{8}$$

where ΔV represents the change in partial molar volume of the solute associated with its passage between the stationary and the mobile phase. At constant temperature,

$$\left(\frac{\partial \Delta G}{\partial P}\right)_T = \Delta V \tag{9}$$

The validity of Eq. (9) relies on the assumptions that there are no solute–solute interactions and that the volume of the system is constant. The change in partial molar volume of the solute can be estimated from a graph of the logarithm of the retention factor versus the pressure at constant temperature, provided that the phase ratio remains constant. The pressure dependence of the other constants defined earlier is given by:

$$\left(\frac{\partial \ln K}{\partial P}\right)_T = -\frac{\Delta V}{RT} \tag{10}$$

$$\left(\frac{\partial \ln q_s}{\partial P}\right)_T = -\frac{\Delta V_{q_s}}{RT} \tag{11}$$

$$\left(\frac{\partial \ln b}{\partial P}\right)_T = -\frac{\Delta V_b}{RT} \tag{12}$$

where ΔV_b and ΔV_{q_s} are the contributions to the partial molar volume change associated with the affinity or apparent equilibrium constant and with the number of adsorption sites (see Eq. (3)), respectively.

2.2. Adsorption equilibrium isotherms

In a chromatographic system, the behavior of the solute is characterized by the equilibrium isotherm or relationship between the concentrations of this compound in the stationary and mobile phase at equilibrium. At high solute concentrations, the isotherm deviates almost always from a linear relationship. The surface of the stationary phase is heterogeneous because the pore structure of the silica is not homogeneous and neither is the ligand distribution on its surface nor the structure of the protein itself. Accordingly, an isotherm model for heterogeneous

surfaces is expected best to model the isotherm data. Because the degree of solvation of the stationary phase is expected to change with pressure as well as that of the protein molecule, the energy distribution will also change with pressure and so will the coefficients of the isotherm model. Among the isotherm models used in chromatography to account for the behavior of non-homogeneous surfaces, the Langmuir–Freundlich and the Toth models are the simplest and most popular.

The Langmuir model is

$$q = \frac{q_s bC}{1 + bC} \tag{13}$$

where q is the amount adsorbed at equilibrium with the concentration C in the solution, q_s is the saturation capacity, and b is the equilibrium constant of adsorption.

There are several models to account for adsorption on heterogeneous surfaces. The simplest such model assumes that the surface is a mixture (patchwork) of two homogeneous surfaces, consisting, e.g., of two different kinds of chemical groups behaving independently. The equilibrium isotherm is the addition of two independent contributions corresponding to the two types of adsorption sites. The bi-Langmuir isotherm [28] was used successfully to account for adsorption data in gas chromatography and HPLC, particularly for enantiomers [29–32]. The equation of this model is

$$q = \frac{q_{s1} b_1 C}{1 + b_1 C} + \frac{q_{s2} b_2 C}{1 + b_2 C} \tag{14}$$

where the subscripts 1 and 2 refer to the two types of adsorption sites.

The Langmuir–Freundlich and the Toth models have one more parameter that accounts for the surface heterogeneity. The equation of the Langmuir–Freundlich isotherm is:

$$q = \frac{q_s (bC)^{\nu}}{1 + (bC)^{\nu}} \tag{15}$$

where ν is the dimensionless heterogeneity parameter. The equation of the Toth isotherm model is:

$$q = \frac{q_s bC}{[1 + (bC)^{\nu}]^{1/\nu}} \tag{16}$$

The Toth exponent, ν, is between 0 and 1, with 1 corresponding to a homogeneous surface while numbers close to 0 correspond to strongly heterogeneous surfaces.

2.3. Lumped pore diffusion model (POR)

This model of chromatography considers separately the mobile phase stream percolating through the packed bed of the column and the stagnant mobile phase contained inside the pores of the particles of the packing material. It further considers the rate of the mass transfer kinetics between these two liquid phases and the equilibrium between the stagnant liquid phase and the stationary phase. The mass balance of a component of the mobile phase in the stream is written:

$$\varepsilon_e \cdot \frac{\partial C_i}{\partial t} + u \cdot \frac{\partial C_i}{\partial z} =$$

$$\varepsilon_e D_L \cdot \frac{\partial^2 C_i}{\partial z^2} - (1 - \varepsilon_e) k_i a_p (C_i - \overline{C}_{p,i}) \tag{17}$$

The mass balance of this compound in the pores of the solid-phase is

$$\varepsilon_p \cdot \frac{\partial \overline{C}_{p,i}}{\partial t} + (1 - \varepsilon_p) \cdot \frac{\partial \overline{q}_i}{\partial t} = k_i a_p (C_i - \overline{C}_{p,i}) \tag{18}$$

where $\overline{C}_{p,i}$ and $\overline{q}_i$ denote the average over the particle of the concentrations in the stagnant liquid and in the stationary phase, respectively, k_i is the overall mass transfer coefficient for component i, ε_e is the external porosity, t is the time, z is the abscissa along the column, u is the superficial mobile phase velocity, D_L is the axial dispersion coefficient, and a_p is the ratio of the absorbent particle external surface area to its volume. For an n-component sample, we have a system of $2n$ partial differential equations. Its integration requires a set of initial and boundary conditions that describe in mathematical terms the experiment that is actually carried out.

2.3.1. Initial conditions

At the beginning of the experiment, the column contains a certain concentration distribution along its length, depending on the experiments previously done. Hence

$$\overline{C}_{p,i} = C^0_{p,i}; \overline{q}_i = q^0_i(z) \quad (19)$$

In most cases, the column is empty of sample components at the beginning of the separation and all the concentrations C^0_i are equal to zero.

2.3.2. Boundary conditions for the mass balance equations

The boundary conditions at the column inlet and outlet are the conventional Dankwerts conditions that take into account axial dispersion of the feed components at their entrance into the column. The condition for $t > 0$, $z = 0$ is given as:

$$u_f C_{f,i} = uC_i - \varepsilon_e D_L \cdot \frac{\partial C_i}{\partial z} \quad (20)$$

$$\begin{aligned} C_{f,i} &= C^0_{f,i} \quad \text{for } 0 < t < t_p \\ C_{f,i} &= 0 \quad \text{for } t_p < t \end{aligned} \quad (21)$$

The condition for $t > 0$ and $z = L$ is

$$\frac{\partial C_i}{\partial z} = 0 \quad (22)$$

Combined with the mass balance equations and the equilibrium isotherm, these equations constitute the mathematical translation of the POR model.

2.4. Calculation of the numerical solutions

The system of equations of the POR model was solved numerically using a program based on the method of orthogonal collocation on finite elements [31–35]. The set of discretized ordinary differential equations obtained in this method was solved with the Adams–Moulton method implemented following the VODE procedures [36]. The relative and absolute tolerance parameters used to control the error in the calculation of the concentrations were 1×10^{-6} and 1×10^{-8}, respectively.

3. Experimental

3.1. Equipment

A HP 1100 liquid chromatography system (Agilent Technologies, Palo Alto, CA, USA) was used for all experimental determinations. This instrument was equipped with a multi-solvent delivery system, an automatic sample injector with a 100-μl loop, a diode-array detector, a high pressure flow cell and a computer data station.

Two characteristics of this instrument are critical for the success of the experiments made and reported here. Firstly, its pumping system is extremely stable. The flow-rate delivered has a long term stability that proved to have a reproducibility better than 0.1%. The mobile phase for the breakthrough measurements was obtained by mixing two solvents in appropriate proportions (see later). The stability of the composition of this binary solution was also better than 0.1% [37]. The pumping system was also used to deliver large but accurately known volumes of samples to the column when needed. Secondly, the pressure in the cell of the UV detector can be as high as 400 bar if needed. There was no adverse effects and the response was not affected.

3.2. Chromatographic conditions

3.2.1. Mobile phase and chemicals

The mobile phase was a solution of acetonitrile–water (30:70, v/v) with 0.1% trifluoroacetic acid. Acetonitrile and water were HPLC grade solvents from Fisher Scientific (Fair Lawn, NJ, USA). Porcine insulin (M_r 5778, isoelectric point, pI = 6.0) and Lispro were gifts from Eli Lilly (Indianapolis, IN, USA). Lispro is an analog of human insulin in which the residues B28 and B29 are reversed. The insulin variants were at a purity of 99%, determined through a HPLC assay. Trifluoroacetic acid (TFA) was from Across (NJ, USA). PTFE filters (pore size 0.2 μm) were purchased from Nalgene (Rochester, NY, USA).

All the samples used in the experiments reported here were freshly prepared and filtered completely to remove any suspended particles.

3.2.2. Column

The column used in our experiments was a YMC ODS-A column (Waters, Milford, MA, USA), with dimensions 150 × 3.9 mm (column no. EJ11490). The particle size of the stationary phase was 5 μm with an average pore diameter of 12 nm. The column had a hold-up volume of 1.08 ml and a stationary phase volume of 0.71 ml. The volume between the

pump outlet and the detector measured with a zero-dead volume connector, without a column, was 0.80 ml. To raise the average column pressure while keeping constant the mobile phase flow-rate, a section of ca 0.0625 mm (exactly, 0.0025 in.) I.D. polyether ether ketone (PEEK) tubing of appropriate length was connected to the outlet of the detector. The pressure drop across the column remained practically unchanged (the compressibility of the mobile phase is negligible) but the whole column was subject to a higher pressure, up to 240 bar in this work. A length of tubing of ~45 cm raises the outlet column pressure from atmospheric to 200 bar at a flow-rate of 1 ml/min. Changes in this length in order to operate at different flow-rates or to achieve different outlet pressures are proportional.

3.3. Procedures for the determination of the isotherm

The equilibrium isotherms were measured by frontal analysis. A staircase series of breakthrough curves was generated as described elsewhere [26], at a constant flow-rate of 1 ml min^{-1}. The two pumps of the chromatographic system were used to deliver a mixture of the pure mobile phase and of the sample solution in the mobile phase having the desired composition. A series of streams of increasing concentration was generated by using the step-gradient function of the solvent delivery system. Each data point of an isotherm was measured twice. The average value is reported.

After each series of measurements, the column was regenerated to remove any adsorbed material. This was done by gradient elution, using a solution of 0.1% TFA in acetonitrile–water (30:70, v/v) as solution A and a solution of 0.1% TFA in acetonitrile–water (50:50, v/v) as solution B, with a gradient time of 20 min at a flow-rate of 1 ml min^{-1}. The column was then re-equilibrated at the initial conditions for another measurement.

4. Results and discussion

4.1. Adsorption equilibrium isotherms

A series of frontal analysis experiments was carried out to determine the adsorption isotherms of insulin variants under different column pressures. The experimental adsorption data acquired were fitted to the equations of the Langmuir, the bi-Langmuir, the Langmuir–Freundlich, and the Toth models (Eqs. (13)–(16)). The best values of these parameters are listed in Tables 1 and 2. The Toth and the bi-Langmuir equations provided the best fit (see Figs. 1 and 2).

Our experimental results and the fact that the data fit well to conventional isotherm models (Langmuir, bi-Langmuir, and Toth) demonstrate that the adsorption and desorption of insulin are reversible under the conditions of our study. This situation is different from the one encountered, for example, in the study of the adsorption of insulin on a hydrophobic methylated silica surface in 4-(2-hydroxyethyl)-1-piperazine ethanesulfonic acid (HEPES) buffer, at pH 7.0, a phenomenon that was shown not to be reversible [38]. In the presence of acetonitrile, the hydrophobicity of insulin and that of the C_{18} stationary phase are reduced.

The data demonstrate that the saturation capacities of the insulin variants increase markedly with increasing pressure. The Langmuir saturation capacity of the column increases by 50% (Table 1). The saturation capacity derived from the Toth model increases more but this result may be less accurate and is more difficult to interpret. An increase in the column saturation capacity means that, at constant mobile phase concentration, the fractional surface coverage decreases with increasing pressure. Better to understand this important result and to ascertain that it reflects the true potential of the column for protein separations, and not just some spurious result of the calculation procedure of fitting the data, we need to analyze the absolute surface coverage of the solute and the monolayer adsorption capacity of the stationary phase.

Let us define a monolayer relative density, δ, as the ratio of the surface occupied by the molecules forming a monolayer coverage of the surface to the surface area of the adsorbent (usually measured by nitrogen adsorption or by mercury porosimetry). This relative density is given by:

$$\delta = \frac{A_m}{A_s} = \frac{1000\, N_A q_s A_c}{M_r S d} \tag{23}$$

Table 1
Best adsorption isotherm parameters for Lispro

Average pressure (bar)	Parameters of isotherm models		
	Langmuir	Bi-Langmuir	Toth
56.5	$q_s = 15.71 \pm 0.52$ (g/l) $b = 0.544 \pm 0.034$ (l/g)	$q_{s1} = 3.15 \pm 0.35$ (g/l) $b_1 = 2.340 \pm 0.176$ (l/g) $q_{s2} = 20.08 \pm 1.18$ (g/l) $b_2 = 0.187 \pm 0.027$ (l/g)	$q_s = 31.01 \pm 2.07$ (g/l) $b = 0.411 \pm 0.02$ (l/g) $n = 0.557 \pm 0.018$
118.5	$q_s = 16.66 \pm 0.43$ (g/l) $b = 0.576 \pm 0.029$ (l/g)	$q_{s1} = 1.24 \pm 0.33$ (g/l) $b_1 = 4.934 \pm 1.05$ (l/g) $q_{s2} = 17.62 \pm 0.44$ (g/l) $b_2 = 0.391 \pm 0.039$ (l/g)	$q_s = 32.23 \pm 1.86$ (g/l) $b = 0.439 \pm 0.018$ (l/g) $n = 0.563 \pm 0.016$
178.5	$q_s = 18.51 \pm 0.66$ (g/l) $b = 0.620 \pm 0.045$ (l/g)	$q_{s1} = 2.84 \pm 2.04$ (g/l) $b_1 = 3.587 \pm 2.15$ (l/g) $q_{s2} = 21.57 \pm 3.64$ (g/l) $b_2 = 0.273 \pm 0.15$ (l/g)	$q_s = 46.27 \pm 15.26$ (g/l) $b = 0.442 \pm 0.090$ (l/g) $n = 0.475 \pm 0.074$
237.5	$q_s = 21.78 \pm 0.95$ (g/l) $b = 0.640 \pm 0.056$ (l/g)	$q_{s1} = 4.01 \pm 0.62$ (g/l) $b_1 = 3.74 \pm 0.47$ (l/g) $q_{s2} = 28.69 \pm 2.92$ (g/l) $b_2 = 0.209 \pm 0.047$ (l/g)	$q_s = 62.51 \pm 7.5$ (g/l) $b = 0.461 \pm 0.035$ (l/g) $n = 0.431 \pm 0.022$

where A_m is the total surface area occupied by the adsorbed solute in the monolayer, A_s is the surface area of the stationary phase, q_s is the saturation capacity of the adsorbent in the column, M_r is the molecular mass of the solute adsorbed on the column, N_A is Avogadro's number, A_c is the maximum cross-section area of the solute molecule, d is the packing density of the stationary phase, and S is the specific surface area of the stationary phase.

The difference between the values derived for small molecules and for insulin on the same or a similar packing material is striking. For example, for

Table 2
Best adsorption isotherm parameters for porcine insulin

Average pressure (bar)	Parameters of isotherm models and Fisher ratio		
	Langmuir	Bi-Langmuir	Toth
56.5	$q_s = 14.80 \pm 0.43$ (g/l) $b = 0.709 \pm 0.043$ (l/g)	$q_{s1} = 4.43 \pm 1.07$ (g/l) $b_1 = 2.244 \pm 0.36$ (l/g) $q_{s2} = 17.38 \pm 2.76$ (g/l) $b_2 = 0.198 \pm 0.086$ (l/g)	$q_s = 23.74 \pm 1.80$ (g/l) $b = 0.639 \pm 0.033$ (l/g) $n = 0.610 \pm 0.028$
118.5	$q_s = 17.15 \pm 0.71$ (g/l) $b = 0.674 \pm 0.058$ (l/g)	$q_{s1} = 3.99 \pm 1.41$ (g/l) $b_1 = 2.828 \pm 0.72$ (l/g) $q_{s2} = 20.99 \pm 4.26$ (g/l) $b_2 = 0.214 \pm 0.11$ (l/g)	$q_s = 33.84 \pm 4.3$ (g/l) $b = 0.563 \pm 0.047$ (l/g) $n = 0.530 \pm 0.035$
178.5	$q_s = 19.67 \pm 0.77$ (g/l) $b = 0.694 \pm 0.057$ (l/g)	$q_{s1} = 4.63 \pm 0.63$ (g/l) $b_1 = 3.153 \pm 0.33$ (l/g) $q_{s2} = 26.17 \pm 2.97$ (g/l) $b_2 = 0.191 \pm 0.047$ (l/g)	$q_s = 44.23 \pm 4.2$ (g/l) $b = 0.571 \pm 0.035$ (l/g) $n = 0.483 \pm 0.022$
237.5	$q_s = 22.37 \pm 1.1$ (g/l) $b = 0.683 \pm 0.070$ (l/g)	$q_{s1} = 5.16 \pm 0.64$ (g/l) $b_1 = 3.678 \pm 0.39$ (l/g) $q_{s2} = 36.98 \pm 7.30$ (g/l) $b_2 = 0.139 \pm 0.047$ (l/g)	$q_s = 72.76 \pm 15$ (g/l) $b = 0.514 \pm 0.061$ (l/g) $n = 0.393 \pm 0.032$

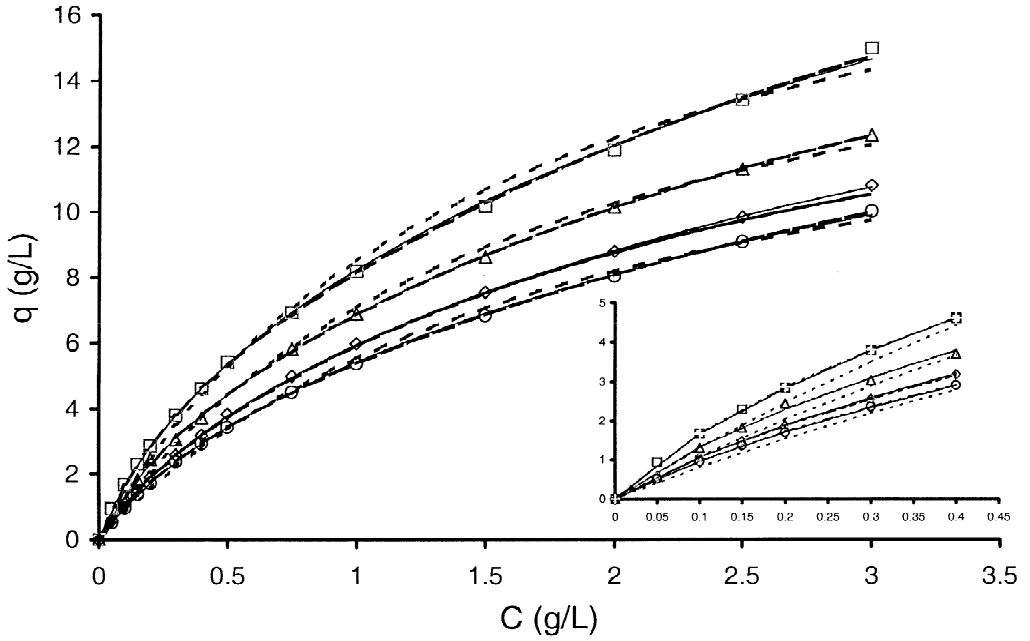

Fig. 1. Experimental adsorption data (symbols) and best fit isotherms of Lispro. ○, 56.5 bar; ◇, 118.5 bar; △, 178.5 bar; □, 237.5 bar. Best fit isotherms: -- -- -- Langmuir; – – – bi-Langmuir; —— Toth.

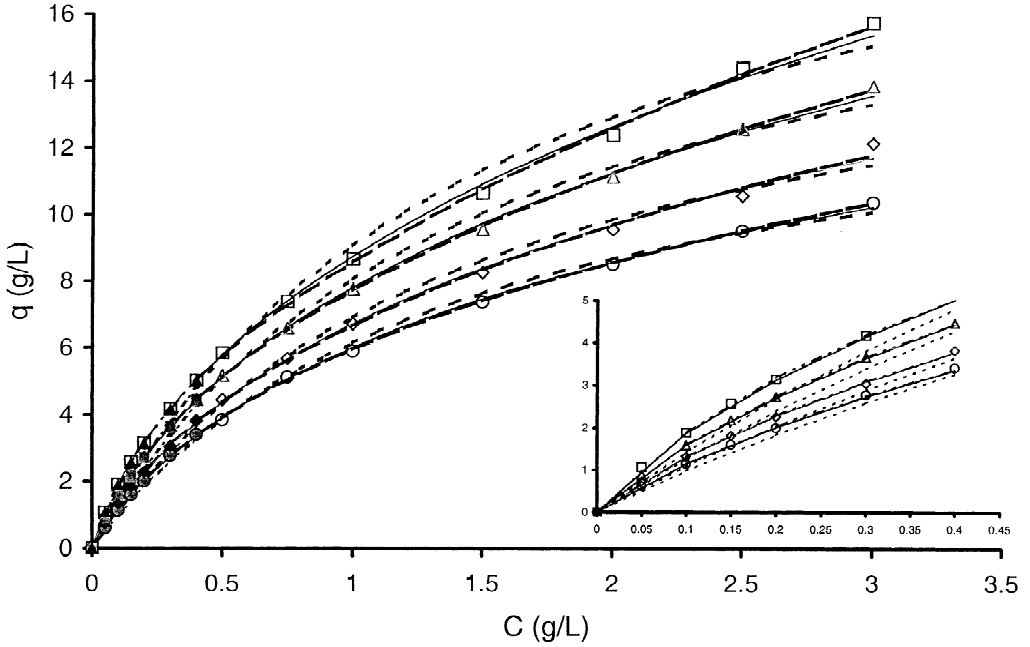

Fig. 2. Experimental adsorption data (symbols) and best fit isotherms of porcine insulin. ○, 56.5 bar; ◇, 118.5 bar; △, 178.5 bar; □, 237.5 bar. Best fit isotherms: -- -- -- Langmuir; – – – Bi-Langmuir; —— Toth.

3-phenyl-1-propanol, the values of δ are 0.49 and 1.1 on a column packed with Symmetry C_{18} (Waters) and on a Chromolith Performance monolithic C_{18} column (Merck, Darmstadt, Germany), respectively [39]. For alprenolol, propranolol, and metoprolol on immobilized CBH I, these values are 0.46, 0.69, and 0.32, respectively [40,41]. For 1-phenyl-1-propanol on cellulose tribenzoate coated on silica, the value of δ is 0.91 [42]. By contrast, using an average value of the saturation capacity for insulin of 20 g/l (see Table 2), we find for insulin on a conventional C_{18} silica, a value of δ equal to 0.014. This shows that the monolayer is not compact. Changes in the experimental conditions should be expected to affect strongly the saturation capacity. Previous results by Sabharwal and Chase [43] have shown that the saturation capacity of bovine insulin on the silica-based BioPrep C4 (Whatman, Clifton, NJ, USA) decreases from 21.9 to 3.4 mg/g when the acetonitrile concentration in the mobile phase increases from 30 to 36%.

Because the compressibility of the insulin molecule is small, the relative decrease of its diameter upon an increase of the average column pressure of several hundred bars is small. The relative compression of insulin is 0.35% under 14.7 kbar and probably linear in between [44]. It is thus of the order of 0.005% under our experimental conditions. This value is very small. Accordingly, the surface area of the micropores, an area which is not accessible for insulin under normal conditions, is still not accessible for insulin under the highest pressure used in this work. This implies that the increase of the saturation capacity with increasing pressure does not arise from an increase of the surface area of the stationary phase that is available for the insulin molecules. It rather arises from changes in the surface topography, in the chemistry of the stationary phase surface, and/or in the binding area of the insulin molecules.

The best values obtained for the affinity constant b and the heterogeneity coefficient n of the Toth isotherm models for Lispro and porcine insulin decrease with increasing column pressure (see Tables 1 and 2). This result indicates that the heterogeneity of the surface increases with increasing pressure. It is confirmed by the pressure variation of the affinity distribution (not shown). Because of its size (approximate dimensions, $20\times20\times25$ Å) relative to that of the ligands (length of the C_{18} alkyl chain: 17 Å) which are bonded to the silica substrate, insulin tends to interact mostly with the end of the bonded alkyl chains opposed to their bond with silica. The weakening of the ionic and hydrophobic interactions binding insulin to the surface that is indicated by the pressure dependence of the affinity constant may be caused by a change in the solvation of the stationary phase and/or of the local conformation of the insulin binding sites.

Protein stability, association, binding to ligands, and catalytic activity all depend on the structure of the protein that is greatly influenced by the properties of the solvent [45]. Solvent and/or water molecules interact with the groups at the surface of the protein and provide a solvation shell. Some such molecules may occupy cavities inside the protein structure, stabilizing it. Others, bound to the surface contribute to the stability of the structure. Chains and clusters of solvent molecules are a distinct feature of the protein surface and modulate the dynamic properties of protein segments. X-ray crystallography of the insulin crystals obtained in the presence of 20% acetic acid shows that the group of residues in B25–B30, at the C-terminal of the B-chain, is highly flexible when not involved in a dimer formation [46]. The data for residues B21–B25 indicate multiple conformations of this part of the molecule. The isolated B-chain adopts the same characteristic structure that it has in intact insulin without the need for extensive cooperative interactions with the A-chain and its C-terminal appears significantly more mobile. In a 20% acetic acid solution, evidence for an equilibrium among conformational substates is provided by the observation of large variations in the amide line-widths observed in two-dimensional NMR, which suggests intermediate exchanges among these substates [47,48]. The residues B24–28 adopt an extended configuration in the monomer and the residues B29 and B30 are largely disordered. The flexibility in the C-terminal region of the B-chain plays a functional role. It undergoes a considerable conformation change upon binding to the receptor.

NMR and electron spin resonance spectrometry (ESR) measurements [49,50] have shown that the solvation environment of the bonded phase depends much on the microstructure of the solution. The

polarity of the solvation layer of alkyl bonded phases depends also on the composition of the mobile phase [51]. Motional behavior is heterogeneous along the alkyl chain [52]. The effect of organic modifiers on the ligand mobility is stronger for the methylene groups located near the end of the chain than for those close to the silica surface [53,54]. The freedom of translational and conformational dynamics are larger at the chain free end for both monomeric and polymeric bonded phases [52,55].

X-ray diffraction and infrared spectroscopy studies of acetonitrile–water mixtures suggest that hydrogen bonds are formed between acetonitrile and water molecules in mixtures with an acetonitrile mole fraction, $X_{AN} \leq 0.8$ [56]. At high water contents ($X_{AN} \leq 0.2$), the acetonitrile clusters are broken and water clusters become predominant. For the mobile phase used in our work, the range of acetonitrile concentration is between 28% and 36%, corresponding to acetonitrile mole fractions between 0.117 and 0.161. Thus, the mobile phase that we used contains water clusters but no acetonitrile ones.

In conclusion, the influence of pressure on the characteristics of the adsorption equilibrium of insulin under the experimental conditions used in this work is mediated by the influence of pressure on the solvation layer of the stationary phase and on the solvation shells of the insulin molecule [25]. Pressure enhances the degree of solvation, hence the configurational reorientation of the alkyl chain segments of the stationary phase and the configurational substates of the C-terminal part of the B-chain. Although the distribution constant of insulin between the two phases of the chromatographic system increases with increasing pressure, the affinity constant decreases for porcine insulin and increases for Lispro (Tables 1 and 2). The increase of the term $[D]$ outweighs the decrease of the affinity constant [25]. The increase of the column saturation capacity correlates with the increase of the number of adsorption sites (Fig. 3).

4.2. Validation of the column saturation capacity under different pressure

The values of the column saturation capacity calculated by fitting the adsorption data obtained under different column pressures to several equilibrium models depend on the model used. Accordingly, because the column saturation capacity controls the production rate of purified compound that can be achieved in preparative liquid chromatography, we felt it necessary to find out which model represents best the actual properties of the column. A series of experiments was carried out under the same loading factor, 1.8% for the Toth model and 2% for the bi-Langmuir model. The actual sample size was increased with increasing pressure in order to keep the loading factor constant. Figs. 4 and 5 show the

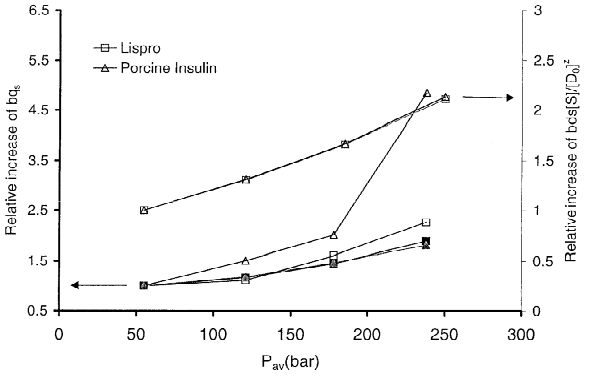

Fig. 3. Relative increase of $b_{ds}[S]/[D_0]^Z$ under linear conditions and of bq_s derived from the Toth and the bi-Langmuir isotherms of insulin. Toth isotherm: □, Lispro; △, porcine insulin. Bi-Langmuir isotherm: ■, Lispro; ▲, porcine insulin.

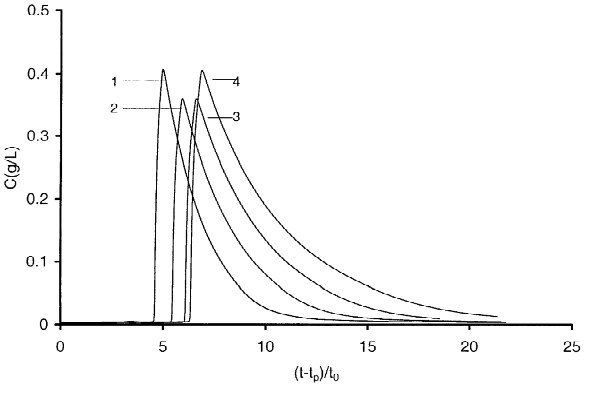

Fig. 4. Overloaded band profiles of porcine insulin under different column pressures. Injection volume, 1 ml. Loading factor, 2% (derived from a column saturation capacity estimated from the best coefficients of the bi-Langmuir isotherm model). Average column pressure and concentration of insulin: 1, 56.5 bar, 0.96 g/l; 2, 118.5 bar, 1.1 g/l; 3, 178.5 bar, 1.36 g/l; 4, 237.5 bar, 1.85 g/l.

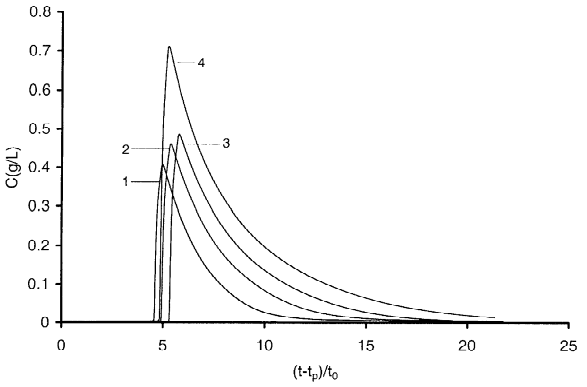

Fig. 5. Overloaded band profiles of porcine insulin under different column pressures. Injection volume, 1 ml. Loading factor, 1.8% (derived from a column saturation capacity estimated from the best coefficients of the Toth isotherm model). Average column pressure and the concentration of insulin: 1, 56.5 bar, 0.96 g/l; 2, 118.5 bar, 1.37 g/l; 3, 178.5 bar, 1.79 g/l; 4, 237.5 bar, 2.94 g/l.

overloaded profiles of porcine insulin recorded under different pressures. The experimental results indicate that the value of the column saturation capacity derived from the best bi-Langmuir model is the more likely to reflect the actual behavior of the overloaded column when the pressure is increased. The saturation capacity is doubled for a 180 bar increase of the average column pressure. It seems that the Toth isotherm model tends to overestimate the actual value of the saturation capacity.

4.3. Partial molar volume change and the adsorption isotherm

The partial molar volume change, ΔV, was previously measured under linear conditions [25]. The contributions to this partial molar volume change related to the affinity constant and the number of binding sites, i.e. the saturation capacity, were derived from the adsorption isotherm data measured under different pressure, using Eqs. (10)–(12). Table 3 listed the values of volume change contributions estimated from the Langmuir and Toth isotherms. For the two insulin variants, the values estimated from the Langmuir isotherm are in reasonably good agreement. However, the value derived from the Toth isotherm for porcine insulin is much higher than that obtained from the Langmuir isotherm. For Lispro, it was not even possible to derive precise estimates of these quantities with the Toth isotherm.

Table 3
Volume change of insulin estimated from the retention factor and the adsorption isotherm

	Parameter	Lispro (ml/mol)	Porcine insulin (ml/mol)
Langmuir	b	−23.7	5
	q_s	−44.6	−56.5
	bq_s	−68.2	−53
Toth	b	–	+
	q_s	–	−148.2
	bq_s	–	−81.06

Fig. 6 shows the influence of pressure on the ratio of the initial slope of the isotherm, Fbq_s, and the column retention factor determined under linear conditions. This ratio should be equal to 1, as it is, within experimental errors, with the bi-Langmuir isotherm model. With the other two models considered, the Langmuir and Toth models, it decreases with increasing pressure for both insulin variants.

4.4. Modeling of band profiles recorded under different pressures

Providing the highest value of the Fisher coeffi-

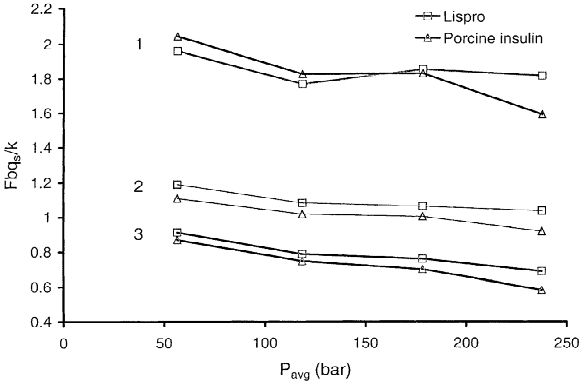

Fig. 6. Influence of pressure on the ratio of Fbq_s derived from the different adsorption isotherms and the retention factor under linear conditions. □, Lispro; △, porcine insulin. (1) The Toth isotherm. (2) The bi-Langmuir isotherm. (3) The Langmuir isotherm.

Table 4
Parameters used in the POR model

Parameter	Value
Molecular diffusion coefficient, D_m (cm^2/min)	6.72×10^{-5}
Effective diffusion coefficient, D_{eff} (cm^2/min)	5.5×10^{-6}
Dispersion coefficient, D_L (cm^2/min)	7.44×10^{-3}
External mass transfer coefficient, k_{ext} (cm/min)	1.55
Internal mass transfer coefficient, k_{int} (cm/min)	0.11
Total porosity, ε_t	0.603
External porosity, ε_e	0.37
Internal porosity, ε_p	0.37

cient, the Toth model is the model to which the experimental data fit best. It was used to calculate the breakthrough curves of frontal analysis and the profiles of overloaded bands. Table 4 lists the parameters used in the calculations. Fig. 7 shows a comparison of calculated and experimental band profiles of porcine insulin at different pressures. The agreement between the two sets of profiles indicates that the chromatographic behavior of insulin is mainly controlled by the equilibrium thermodynamics. The mass transfer kinetics seem to be relatively fast and almost independent of the average column pressure.

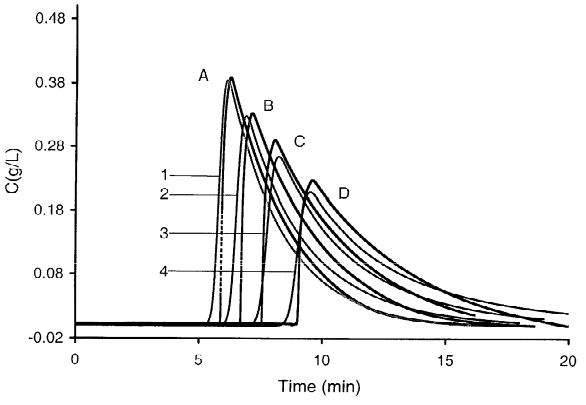

Fig. 7. Comparison of the experimental overloaded band profiles of a large sample of porcine insulin under different average column pressures and the profiles calculated using the POR model. Injection volume, 1 ml; concentration, 1 g/l. The solid lines labeled 1, 2, 3 and 4 correspond to the profiles calculated with the POR model under different pressures. Dashed line, experimental data; solid lines, calculated profiles. A, 56.5 bar; B, 118.5 bar; C, 178.5 bar; D, 237.5 bar.

5. Conclusion

The main result of this work is the demonstration of a rapid increase of the column saturation capacity with increasing average column pressure. This effect is primarily related to the large value of the change, ΔV, in the partial molar volume of the protein associated with its adsorption. Since proteins have a large molar volume, it is not surprising that ΔV, although rather modest in relative value, is important enough to cause pressure to affect all the parameters of the isotherm. For insulin, the molar volume is of the order of 4500 ml and ΔV is -100 ml/mol, a 2% change. Yet, it is enough to explain a twofold increase of the retention factor and a similar change in the saturation capacity when the average column pressure is increased by 180 bar. Pressure has also a strong influence on the solvation layer of the alkyl-bonded stationary phase, the solvation shell of the hydrophobic regions of the protein, and the hydration shell of the hydrophilic parts of the protein.

Accordingly, we may anticipate a similar influence of pressure on the retention of most proteins, at least in RPLC. It is noteworthy that the distribution coefficients of insulin variants increase with increasing pressure whereas the affinity constants b decrease. The association constant b_{ds}, which characterizes the adsorption/desorption equilibrium of insulin in the chromatographic system increases with increasing pressure and the parameter characterizing the surface heterogeneity decreases. This suggests that the surface of the stationary phase becomes more heterogeneous. It seems that the pressure-induced increase of the number of adsorption sites is the major cause of the observed increase of the saturation capacity.

Finally, the excellent agreement between calculated and experimental band profiles recorded under different pressures suggests that the mass transfer kinetics is relatively fast and nearly independent of the average column pressure.

Acknowledgements

This work was supported in part by grant CHE-00-70548 of the National Science Foundation, and by

the cooperative agreement between the University of Tennessee and the Oak Ridge National Laboratory.

References

[1] K. Heremans, in: R. Winter, J. Jonas (Eds.), High Pressure Chemistry, Biochemistry and Materials Science, Kluwer Academic, Dordrecht, 1993, p. 443.
[2] M. Gross, R. Jaenicke, Eur. J. Biochem. 221 (1994) 617.
[3] V.V. Mozhaev, K. Heremans, J. Frank, P. Masson, C. Balny, Proteins Struct. Funct. Genet. 24 (1996) 81.
[4] C. Balny, P. Masson, K. Heremans, Biochim. Biophys. Acta 1595 (2002) 3.
[5] R.I. St. John, J.F. Carpenter, T.W. Randolph, PNAS 96 (1999) 13029.
[6] H. Frauenfelder, N.A. Alberding, A. Ansari, D. Braunstein, B.R. Cowen, M.K. Hong, I.E.T. Iben, J.B. Johnson, S. Luck, M.C. Marden, J.R. Mourant, P. Ormos, L. Reinisch, R. Scholl, A. Shulte, E. Shyamsunder, L.B. Sorensen, P.J. Steinbach, A. Xie, R.D. Young, K.T. Yue, J. Phys. Chem. 94 (1990) 1024.
[7] K. Heremans, L. Smeller, Biochim. Biophys. Acta 1386 (1998) 353.
[8] L. Smeller, Biochim. Biophys. Acta 1595 (2002) 11.
[9] K. Heremans, P.T.T. Wong, Chem. Phys. Lett. 118 (1985) 101.
[10] G.J.A. Vidugiris, J.L. Markley, C.A. Royer, Biochemistry 34 (1995) 4909.
[11] N. Hillson, J.N. Onuchic, A.E. Garcia, Proc. Natl. Acad. Sci. USA 96 (1999) 14848.
[12] E. Paci, Biochim. Biophys. Acta 1595 (2002) 185.
[13] R.M. Brunne, W.F. van Gunsteren, FEBS Lett. 323 (1993) 215.
[14] K. Heremans, L. Smeller, Biochim. Biophys. Acta 1386 (1998) 353.
[15] A. Priev, A. Almagor, S. Yedgar, B. Gavish, Biochemistry 35 (1996) 2061.
[16] P. Roy, C.M. Roth, M.N. Margolies, M.L. Yarmush, Mol. Immunol. 36 (1999) 1149.
[17] V.L. McGuffin, C.E. Evans, J. Microcol. Sep. 3 (1991) 513.
[18] G. Guiochon, M.J. Sepaniak, J. Chromatogr. 606 (1992) 148.
[19] M.C. Ringo, C. Evans, Anal. Chem. 69 (1997) 4964.
[20] V.L. McGuffin, S. Chen, J. Chromatogr. A 762 (1997) 35.
[21] C.E. Evans, J.A. Davis, Anal. Chim. Acta 397 (1999) 163.
[22] A. Bylina, M. Ulanowicz, Chem. Anal. (Warsaw) 43 (1998) 955.
[23] S. Chen, C. Ho, K. Hsiao, J. Chen, J. Chromatogr. A 891 (2000) 207.
[24] P. Szabelski, A. Cavazzini, K. Kaczmarski, X. Liu, J.V. Horn, G. Guiochon, J. Chromatogr. A 950 (2002) 41.
[25] X. Liu, D. Zhou, P. Szabelski, G. Guiochon, in preparation.
[26] X. Liu, K. Kaczmarski, A. Cavazzini, P. Szabelski, D. Zhou, G. Guiochon, Biotechnol. Prog. 18 (2002) 796.
[27] X. Geng, F.E. Regnier, J. Chromatogr. 296 (1984) 15.
[28] D. Graham, J. Phys. Chem. 57 (1953) 665.
[29] R.J. Laub, ACS Symp. Ser. 297 (1986) 1.
[30] S. Jacobson, S. Golshan-Shirazi, G. Guiochon, J. Am. Chem. 112 (1990) 6492.
[31] G. Guiochon, S.G. Shirazi, A.M. Katti (Eds.), Fundamentals of Preparative and Nonlinear Chromatography, Academic Press, Boston, MA, 1994.
[32] M. Morbidelli, A. Servida, G. Storti, S. Carrà, Ind. Eng. Chem. Fundam. 21 (1982) 123.
[33] K. Kaczmarski, G. Storti, M. Mazzotti, M. Morbidelli, Comput. Chem. Eng. 21 (1997) 641.
[34] K. Kaczmarski, D. Antos, H. Sajonz, P. Sajonz, G. Guiochon, J. Chromatogr. A 925 (2001) 1.
[35] V.J. Villadsen, M.L. Michelsen (Eds.), Solution of Differential Equation Model by Polynomial Approximation, Prentice-Hall, Engelwood Cliffs, NJ, 1978.
[36] P.N. Brown, A.C. Hindmarsh, G.D. Byrne, Ordinary Differential Equation Solver—Procedure, available at http://www.netlib.org.
[37] M. Kele, G. Guiochon, J. Chromatogr. A 830 (1999) 41.
[38] J. Buijs, C.C. Vera, E. Ayala, E. Steensma, P. Hakansson, S. Oscarsson, Anal. Chem. 71 (1999) 3219.
[39] F. Gritti, W. Piatkowski, G. Guiochon, J. Chromatogr. A 978 (2002) 81.
[40] G. Götmar, T. Fornstedt, G. Guiochon, Anal. Chem. 72 (2000) 3908.
[41] G. Götmar, T. Fornstedt, M. Andersson, G. Guiochon, J. Chromatogr. A 905 (2001) 3.
[42] A. Cavazzini, K. Kaczmarski, P. Szabelski, D. Zhou, X. Liu, G. Guiochon, Anal. Chem. 73 (2001) 5704.
[43] A.P. Sabharwal, H.A. Chase, Trans. Ichem E, Part C 77 (1999) 18.
[44] J.L. Markly, D.B. Northrop, C.A. Royer (Eds.), High Pressure Effects in Molecular Biophysics and Enzymology, Oxford University Press, New York, 1996.
[45] R.B. Gregory (Ed.), Protein–Solvent Interactions, Marcel Dekker, New York, 1995.
[46] Y. Zhang, J.L. Wittingham, J.P. Turkenburg, E.J. Dodsen, J. Brange, G.G. Dodsen, Acta Cryst. D58 (2002) 186.
[47] Q.X. Hua, M.A. Weiss, Biochemistry 30 (1991) 5505.
[48] M.A. Weiss, D.T. Nguyen, I. Khait, K. Inouye, B.H. Frank, M. Beckage, E. O'Shen, S.E. Shoelson, M. Karplus, L.J. Neuringer, Biochemistry 28 (1989) 9855.
[49] D.B. Marshall, W.P. McKenna, Anal. Chem. 56 (1984) 2090.
[50] D.M. Bliesner, K.B. Sentell, Anal. Chem. 65 (1993) 1819.
[51] C. Miller, R. Dadoo, R.G. Kooser, J. Gorse, J. Chromatogr. 458 (1988) 255.
[52] D.W. Sindorf, G.E. Maciel, J. Am. Chem. Soc. 105 (1983) 1848.
[53] M.E. McNally, L.B. Rogers, J. Chromatogr. 331 (1985) 23.
[54] R.C. Zeigler, G.E. Macial, J. Am. Chem. Soc. 113 (1991) 6349.
[55] R.K. Gilpin, M.E. Gangoda, Anal. Chem. 56 (1984) 1470.
[56] T. Takamuku, M. Tabata, A. Yamaguchi, J. Nishimoto, M. Kumamoto, H. Wakita, T. Yamaguchi, J. Phys. Chem. B 102 (1998) 8880.